Theoretical Considerations in the $NH_2 + NO$ Reaction

James A. Miller*

Combustion Research Facility, Sandia National Laboratories, Livermore, California 94551-0969

Stephen J. Klippenstein

Department of Chemistry, Case Western Reserve University, Cleveland, Ohio 44106-7078

Received: August 11, 1999; In Final Form: November 5, 1999

We have studied the $NH_2 + NO$ reaction theoretically in order to try to deduce a theoretical "model" that will accurately reproduce both the total rate coefficient $k_T(T)$ and the branching fraction $\alpha(T)$ of the reaction $NH_2 + NO \rightarrow N_2 + H_2O$ (a), $NH_2 + NO \rightarrow NNH + OH$ (b), and $NH_2 + NO \rightarrow N_2O + H_2$ (c), where $k_T = k_a + k_b + k_c$ and $\alpha = k_b/k_T$. The analysis, which makes the RRKM assumption and utilizes conventional transition-state theory for the internal-rearrangement transition states and microcanonical/fixed-J variational transition-state theory for the bond fissions, is discussed at length. The results of the analysis show clearly that $k_T(T)$ is determined almost exclusively by the transition state for the 1,3 hydrogen transfer connecting the initial NH_2NO complex to HNNOH. The branching fraction is sensitive to several features of the potential energy surface, most of them associated with the fragmentation of the various HNNOH complexes into NNH + OH. By adjusting properties of the potential energy surface, we have constructed a theoretical model that predicts results for both $k_T(T)$ and $\alpha(T)$ that are in good agreement with experiment. A variety of sensitivity analyses for the branching fraction indicate that reaction b is most likely thermoneutral to within ±1 kcal/mol. Our prediction of $k_c(T)$ is between 2 and 3 orders of magnitude smaller than values deduced from experiment, suggesting that the experiment may have detected the existence of a fourth channel, HNNO + H, or may have been contaminated by secondary reactions.

Introduction

The Thermal De-NO_x process[1] (i.e., the selective noncatalytic reduction of NO by ammonia) is used extensively on stationary combustion systems to control NO_x emissions. The key to this process is the reaction between NH_2 and NO,[2−7] which has at least three product channels

$$NH_2 + NO \rightarrow N_2 + H_2O \quad \text{(a)}$$

$$\rightarrow NNH + OH \quad \text{(b)}$$

$$\rightarrow N_2O + H_2 \quad \text{(c)}$$

However, under conditions of interest, only the first two are important. The key element in understanding the mechanism of the process (and constructing a satisfactory kinetic model for it) is the extent to which channel (b) can produce free radicals. Reaction b, followed by the sequence

$$NNH \rightarrow N_2 + H$$

$$H + O_2 \rightarrow OH + O$$

$$O + H_2O \rightarrow OH + OH$$

is chain branching, whereas reaction a is chain terminating. The branched chain character of the process is important for predicting a number of its observed properties.[3−5] The most important parameters in determining the rate of chain branching are the branching fraction of the $NH_2 + NO$ reaction, $\alpha(T) = k_b/k_T$, where k_T is the total rate coefficient, and τ_{NNH}, the lifetime of the NNH radical, which dissociates exothermically into $N_2 + H$ by tunneling through a small potential energy barrier (≈8 kcal/mol).

Both $\alpha(T)$ and τ_{NNH} have been controversial in the past. However, recent experimental determinations of $\alpha(T)$[8−10] have allowed Miller and Glarborg[6] to construct a satisfactory chemical kinetic model for Thermal De-NO_x with a value of $\tau_{NNH} = 1.5 \times 10^{-8}$ s. This value of τ_{NNH} is consistent with the upper limit of 0.5 μs set by the experiments of Selgren et al.[11] and with the theoretical predictions of Koizumi et al.[12] However, the temperature dependence of $\alpha(T)$ suggested by experiment and used in the Miller−Glarborg model is not consistent with the most reliable theoretical prediction of this parameter.[13] Therefore, it seems desirable to explore the theoretical prediction of $\alpha(T)$ in more detail.

The $NH_2 + NO$ reaction is remarkable in a number of ways, one of which is that the dominant channel at low temperature (reaction a) involves the breaking of all three chemical bonds in the reactants and the formation of three completely new ones in the products. Melius and Binkley,[14] using BAC-MP4 electronic structure calculations, were the first to identify the mechanism by which this reaction occurs. Subsequently, numerous electronic-structure theorists[15−20] have confirmed their results, although the exact properties of the transition states involved differ somewhat from investigation to investigation. Using this information, it is easy to show that the lifetimes of the intermediate complexes are $\approx 10^{-11}$ s, even at the minimum energy at which they can be formed from $NH_2 + NO$, whereas the time between collisions at temperatures and pressures of interest is $\approx 10^{-10}$ s.[5,21] Therefore, the reaction takes place as a

10.1021/jp992836y CCC: $19.00
Published on Web 02/23/2000

single elementary step without collisions! This is at least qualitatively consistent with the experimental observation that the rate coefficient is independent of pressure from a few Torr to almost an atmosphere at room temperature.[22]

There have not been very many attempts to predict theoretically the kinetic properties of the reaction, i.e., the rate coefficient k_T and product distribution. The early work by Gilbert et al.[23] and Phillips[21] did not address the branching- fraction issue at all. Diau et al.[24] attempted to calculate both $k_T(T)$ and $\alpha(T)$, but they did not treat the "loose" transition states satisfactorily (i.e., the ones for bond fission), and their method did not enforce angular momentum conservation. The latter is potentially very important in this case because of "rotational channel switching."[5,25,26] Rotational channel switching occurs when the product distribution is determined by the competition between a loose transition state and a tight one that is lower in energy. As the angular momentum quantum number J is increased, the centrifugal barrier for the tight transition state grows much faster than that for the loose one. As a result, there is the possibility that high temperatures (high J's) could essentially shut off the low-energy channel, which would likely be dominant at low temperatures.

The analysis of Diau and Smith[13] is the only satisfactory theoretical treatment of the $NH_2 + NO$ reaction to date. It is pivotal to our understanding of the reaction. These investigators both enforced angular momentum conservation rigorously and treated the loose transition states in a satisfactory fashion. Their calculation of $\alpha(T)$ shows that a rapid rise from about 0.1 at room temperature to high values for $T > 1000$ K (consistent with Thermal De-NO_x modeling) is the *expected* result, based on the best potential energy surface information available. However, their $\alpha(T)$ in fact is much too large at temperatures of interest. We believe that this is due, at least in part, to a conceptual error in the Diau−Smith analysis. This point is discussed in context below.

The present investigation is a rather substantial extension and elaboration of the Diau−Smith treatment. We seek to construct a theoretical model that is consistent with the best experimental results available both for $k_T(T)$ and $\alpha(T)$ and is also consistent with the large body of electronic structure theory information that has accumulated. We also identify features of the PES that are most important in determining these parameters. The rate coefficient k_c for the $N_2O + H_2$ channel also comes naturally out of our analysis.

Theory

Potential Energy Surface. The potential energy surface (PES) used in our analysis is depicted diagrammatically in Figure 1. Information about the tight transition states was drawn initially from the electronic structure calculations of Wolf et al.,[17] except for the transition states leading to $N_2O + H_2$ (TS-6 and TS-7), whose properties come from the work of Diau and Smith.[20] We then adjusted the properties of selected transition states, in light of all the electronic structure theory results available, in order to obtain good agreement with experiment for $k_T(T)$ and $\alpha(T)$. These adjustments are discussed in detail below. The well depths of the various isomers shown in Figure 1 are drawn to reflect the theoretical results of Diau and Smith[20] and Walch.[19] However, these well depths do not enter directly into any of our calculations. The Appendix contains a complete list of the transition-state properties for the tight transition states used in our model.

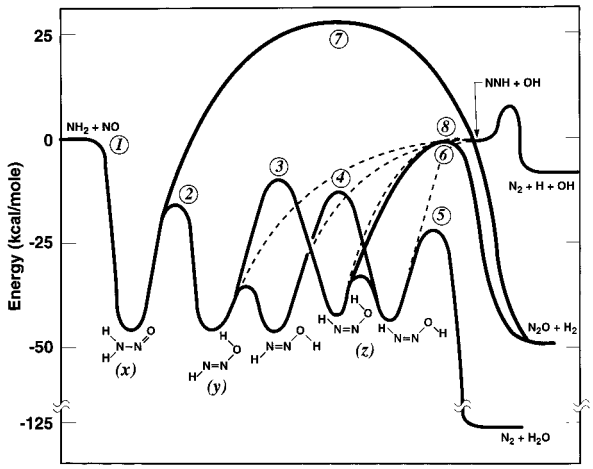

Figure 1. Reaction coordinate diagram for the $NH_2 + NO$ reaction.

For the loose transition states, TS-1 and TS-8, there are no electronic structure calculations from which to draw information. Therefore, we are forced to approximate the potential in these regions of the surface. In doing so, we have separated the potential into three parts: (1) the potential along the reaction coordinate; (2) the potential corresponding to the "conserved" degrees of freedom orthogonal to the reaction coordinate; and (3) the potential for the "transitional" degrees of freedom orthogonal to the reaction coordinate.

For the present investigation we have assumed that the potential along the reaction coordinate can be represented by a Varshni potential[27,28]

$$V(R) = D_e\left\{1 - \frac{R_0}{R}\exp[-\beta(R^2 - {R_0}^2)]\right\}^2 - D_e \qquad (1)$$

where D_e is the "classical" bond energy (i.e., not including zero-point vibrational energies), R the reaction coordinate, and R_0 its equilibrium value. In the present case, R is the distance between the two bonding atoms, the N−N distance for TS-1 and the N−O distance for TS-8.

Note from Figure 1 that TS-8 actually represents four different reaction paths, one leading to each of four isomers of the complex. In the present work, we do not distinguish among these four paths through the $V(R)$ function. There is only one $V(R)$ for TS-8, but the four paths are accounted for properly through the symmetry of the potential for the transitional coordinates. In the end, we calculate the total reactive flux connecting NNH + OH to all four wells of the complex and partition the flux after the fact through an ad hoc parameter (discussed below).

The β parameter in eq 1 can be related to the second derivative of $V(R)$ at R_0

$$\beta = \frac{1}{4R_0}\sqrt{\frac{2V_{RR}(R_0)}{D_e}} - \frac{1}{2{R_0}^2} \qquad (2)$$

$V_{RR}(R_0)$ is readily obtained from electronic structure theory, in the present case from a density functional calculation. Knowing D_e and R_0 from a variety of electronic structure calculations, one can then calculate β from eq 2, i.e., for both TS-1 and TS-8.

We have used the Varshni potential, rather than a Morse function, in our analysis because it is "flatter" at large R. For this reason, the Varshni $V(R)$ is believed to be a more accurate representation of true bonding potentials than is the Morse function.[28] For the same values of D_e, R_0, and $V_{RR}(R_0)$, the

Varshni β is related simply to the Morse β_M

$$\beta = \frac{1}{2R_0}\left(\beta_M - \frac{1}{R_0}\right) \tag{3}$$

For the present case, as noted by Diau and Smith,[13] it does not seem to matter very much which of the two functions is used.

The potential for the conserved coordinates is assumed to be harmonic. This potential corresponds to the degrees of freedom that can be identified as normal-mode vibrations in the separated fragments. The transition states for bond fission reactions normally lie so far out in the asymptotic region of the PES that it is reasonable to assume that these degrees of freedom, and their corresponding frequencies, maintain their integrity in going from the separated fragments to the transition states.

The potential for the transitional coordinates is more complicated. We describe this potential in terms of four angles. For TS-1 these angles are the ONN bond angle, the $H^{(1)}NN$ bond angle (either H can be labeled $H^{(1)}$), and two torsional angles: (1) the dihedral angle between the NH_2 plane and the $H^{(1)}NN$ plane, and (2) the dihedral angle between the $H^{(1)}NN$ plane and the NNO plane. For TS-8 the angles are the $H^{(1)}ON$ bond angle, the NNO bond angle, and two torsional angles: (1) the dihedral angle between the $H^{(2)}NN$ plane and the NNO plane, and (2) the dihedral angle between the $H^{(1)}ON$ plane and the NNO plane.

The transitional potential for either loose transition state can be written compactly in the form

$$V_t(\theta_1,\theta_2,\theta_3,\theta_4) = \sum_{i=1}^{4}\sum_{j\neq i}^{4} A_{ij} \sin p_i(\theta_i - \theta_{i0}) \sin p_j(\theta_j - \theta_{j0}) + \sum_{i=1}^{4} A_{ii}[1 - \cos p_i(\theta_i - \theta_{i0})] \tag{4}$$

where the θ_i's are the angles described above and the θ_{i0}'s are their equilibrium values. The p_i's come from symmetry, i.e., if $p_i = 1$, there is only one minimum in the potential as θ_i goes from 0 to 2π; if $p_i = 2$, there are two minima, etc. The obvious symmetry condition

$$A_{ji} = A_{ij} \tag{5}$$

leaves 10 coefficients to be specified in order to define the potential completely. For TS-1 we do this by calculating from density functional theory the force constant matrix at the equilibrium position of the stable adduct

$$F_{ij}(R_0) = \left(\frac{\partial^2 V}{\partial\theta_i\,\partial\theta_j}\right)_{R_0,\theta_{i0},\theta_{j0}}, \quad i,j = 1, ..., 4 \tag{6}$$

and assume that $F_{ij}(R)$ decays exponentially with increasing R

$$F_{ij}(R) = F_{ij}(R_0)\exp[-\eta(R-R_0)] \tag{7a}$$

where η is a tightening (or loosening) parameter.

The temperature dependence of the branching fraction α is a sensitive function of the potential in the TS-8 region. To allow for greater flexibility in our modeling of this temperature dependence we employ a two-parameter form for the decay of the force constants in this region

$$F_{ij}(R) = F_{ij}(R_0)\exp[-\eta_a(R-R_0)]; \quad R \le R_b$$
$$= F_{ij}(R_0)\exp[-\eta_a(R-R_0)]\exp[-\eta_b(R-R_b)]; \quad R > R_b \tag{7b}$$

We have chosen $R_b = 2.4$ Å at which to switch on the additional decay term, because in the present case such a value provides the greatest flexibility in modifying the T dependence of α. Furthermore, this separation corresponds at least qualitatively to the region where covalent and long-range interactions are of roughly equal importance. In this region there are significant variations in the potential that cannot be modeled with the current simple model function. In particular, hydrogen bonding and dipole−dipole interactions yield dramatic changes with R in the optimum orientation and interaction strength of the fragments. The addition of an extra decay term for the forces, as in eq 7b, while not allowing for a quantitative reproduction of these phenomena, does at least provide greater flexibility in the modeling of their effects. The parameters η_1, η_{8a}, and η_{8b} are discussed below and are chosen to give realistic values of the rate coefficients for complex formation from the corresponding separated fragments. The calculation of $F_{ij}(R_0)$ then is sufficient to determine the 10 independent elements of the **A** matrix defined in eq 4 for any position along the reaction coordinate, and thus it is sufficient to define V_t everywhere.

Rate Coefficient Calculations. Using methods introduced by Miller, Parrish, and Brown,[29] we treat all the possible rearrangements of the NH_2 + NO collision complex, shown in Figure 1, as a stochastic process, allowing for passage back and forth between the various configurations any number of times. Because the lifetimes of the intermediate complexes are very short, as discussed in the Introduction, the reaction occurs without collisions. Therefore, total energy E and total angular momentum must be conserved explicitly in our analysis. We can write rate coefficient expressions for the three product channels as follows:

$$k_a(T) = [hQ_R(T)g_e(T)]^{-1}\sum_J (2J+1)\int_0^\infty \frac{N_5}{D} N_1N_2(N_3 + N_4)\exp(-E/k_BT)\,dE \tag{8}$$

$$k_b(T) = [hQ_R(T)g_e(T)]^{-1}\sum_J (2J+1)\int_0^\infty N_8\frac{N_1N_2}{D}\{\gamma N_z + (1-\gamma)(N_3+N_4)\}\exp(-E/k_BT)\,dE \tag{9}$$

$$k_c(T) = [hQ_R(T)g_e(T)]^{-1}\sum_J (2J+1)\int_0^\infty \left\{N_6\frac{N_1N_2}{D}(N_3 + N_4) + N_7\frac{N_1}{D}[N_yN_z - (N_3+N_4)^2]\right\}\exp(-E/k_BT)\,dE \tag{10}$$

where

$$D(E,J) = N_2^2N_z + N_x[N_yN_z - (N_3+N_4)^2]$$

$$N_x(E,J) = N_1 + N_2 + N_7$$

$$N_y(E,J) = N_2 + N_3 + N_4 + \gamma N_8$$

$$N_z(E,J) = N_3 + N_4 + N_5 + N_6 + N_7 + (1-\gamma)N_8$$

In these expressions k_B is Boltzmann's constant, h is Planck's constant, T is the temperature, J is the total angular momentum quantum number, and $Q_R(T)$ is the vibrational−rotational−translational partition function of the reactants (not including

electronic or center-of-mass contributions). The function $g_e(T)$ is the electronic partition function of the reactants

$$g_e(T) = 2[2 + 2\exp(-346/RT)] \quad (11)$$

The functions $N_i(E,J)/h$, $i = 1, ..., 8$, represent microcanonical/fixed-J probability fluxes per unit energy through the indicated transition states of Figure 1. They are the same in both directions because of microscopic reversibility. For purely classical reaction-path motion (as assumed here), $N_i(E,J)$ is the sum of states with total angular momentum quantum number equal to J and total energy less than or equal to E. The function $\gamma(T)$ is the fraction of the flux through TS-8 that connects the separated NNH + OH fragments with complex y, shown in Figure 1. Recall that our calculation of $N_8(E,J)$ does not discriminate between the part that correlates with complex y and the part that correlates with complex z. Note from Figure 1 that both complexes y and z consist of two "subcomplexes" connected by small rotational barriers. Our analysis implicitly assumes that in both cases the barriers are small enough that RRKM equilibrium is maintained between the subcomplexes during the course of reaction.

Except for TS-3 and TS-4, the $N_i(E,J)$'s for the tight transition states ($i = 2, ..., 7$) are evaluated exactly in the harmonic-oscillator/rigid-rotor approximation using conventional transition state theory. In most of our calculations we approximate one degree of freedom in TS-3 and TS-4 as a hindered rotation. Note from Figure 1 that TS-3 and TS-4 are connected by an out-of-plane rotation of a hydrogen atom, i.e., by a change of π in the dihedral angle ϕ between the HON plane and the ONN plane. The potential for this HONN torsional motion is approximated by a truncated Fourier cosine series

$$V(\phi) = \upsilon_0 + \upsilon_1 \cos\phi + \upsilon_2 \cos 2\phi + \upsilon_3 \cos 3\phi + \upsilon_4 \cos 4\phi \quad (12)$$

where υ_0 through υ_4 are constants. Four of the constants were determined from the assumed values of the potential at the saddlepoints corresponding to TS-3 and TS-4 and from a density functional calculation of the force constants $d^2V/d\phi^2$ at the same two points, i.e., at $\phi = 0$ and $\phi = \pi$. The fifth constant is used as a free parameter to fix a value for the potential energy barrier V_{3-4} at $\phi = \pi/2$ separating TS-3 from TS-4. Two values were used for this barrier, 4 and 8 kcal/mol.

Once we have the potential we can calculate the classical density of states corresponding to this torsional motion for either transition state as a phase space integral

$$\rho_{cl}^{(t)}(E) = \frac{\sqrt{2I_r}}{h}\int_{\phi_l}^{\phi_u} H(E - V(\phi))[E - V(\phi)]^{-1/2}\, d\phi \quad (13)$$

where $H(x)$ is the Heaviside step function and I_r is the reduced moment of inertia for the torsional motion. For TS-4, $\phi_l = -\pi/2$ and $\phi_u = \pi/2$, whereas for TS-3 the limits on ϕ are from $\pi/2$ to $3\pi/2$. Note that $\phi = 0$ corresponds to TS-4 and $\phi = \pi$ corresponds to TS-3. An estimate of the quantum density of states can be obtained from the Pitzer−Gwinn[30] approximation

$$\rho_q^{(t)}(E) = \rho_{cl}^{(t)}(E)\frac{\rho_q^{(ho)}(E)}{\rho_{cl}^{(ho)}(E)} \quad (14)$$

where $\rho_q^{(ho)}(E)$ and $\rho_{cl}^{(ho)}(E)$ are the quantum and classical harmonic-oscillator state densities calculated for the same saddlepoint force constants as used in computing $\rho_{cl}^{(t)}(E)$. The total vibrational sum of states is obtained by convolving $\rho_q^{(t)}(E)$ with the quantum harmonic state sum for the other vibrational degrees of freedom

$$N_\upsilon(E) = \int_0^E \rho_q^{(t)}(x) N_{\upsilon-1}(E - x)\, dx \quad (15)$$

$N(E,J)$ is then obtained from $N_\upsilon(E)$ as described by Miller, Parrish, and Brown.[29]

The fluxes $N_1(E,J)$ and $N_8(E,J)$ are computed by microcanonical/fixed-J variational transition-state theory,[5] in which there is a different transition-state dividing surface for every E,J combination. The dividing surface is chosen from a one-parameter family of surfaces orthogonal to the reaction coordinate by minimizing the total flux through the surface. For the present investigation we employ methods developed by Klippenstein[31] in calculating these fluxes; this methodology is an extension and generalization of the Wardlaw−Marcus approach.[32,33] We calculate a quantum sum of states, $N_c(E)$, by exact count for the conserved degrees of freedom and a classical density of states $\rho_t(E,J)$, for the transitional degrees of freedom (including external rotation) by a Monte Carlo method;[31] $\rho_t(E,J)$ is the transitional density of states per unit energy with total angular momentum quantum number equal to J. We then obtain $N(E,J)$ by convolution

$$N(E,J) = \int_0^E N_c(E - \epsilon)\rho_t(\epsilon,J)\, d\epsilon \quad (16)$$

The computer code VARIFLEX[34] was used in all our calculations for $N_1(E,J)$ and $N_8(E,J)$.

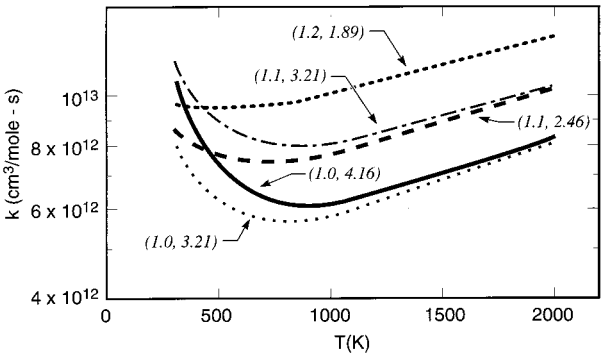

Figure 2. Rate coefficients for the NNH + OH association reaction, $k_8^{(c)}(T)$, for various values of the tightening constants η_{8a} and η_{8b}. The calculations are for cases 1−5. The numbers in parentheses are the values (in Å^{-1}) of η_{8a} and η_{8b}, respectively.

Results and Discussion

The first point we need to address is what to choose for η_1, η_{8a}, and η_{8b}, the tightening parameters for TS-1 and TS-8. The primary criterion that we have is that they should yield reasonable values for the rate coefficients of their corresponding radical association reactions. For TS-1 we have chosen $\eta_1 = 3.0$ Å^{-1}, which results in a value for $k_1^{(c)}$, the rate coefficient for complex formation from NH_2 + NO, of approximately 2.9×10^{13} cm^3/(mol s) at 300 K. This value gradually rises to 4.5×10^{13} cm^3/(mol s) at 2000 K.

We have tried a number of different pairs of η_{8a},η_{8b} values and calculated corresponding values of $k_8^{(c)}$, the rate coefficient (through TS-8) for complex formation from NNH + OH. The results for $k_8^{(c)}(T)$ are shown in Figure 2. At high temperatures the transition state lies at shorter separations than 2.4 Å and the rate coefficient depends only on η_{8a}. At low temperatures,

TABLE 1: Modification to Nominal Potential Energy Surface Parameters

	η_{8a}, η_{8b} ($Å^{-1}$)	$E_0^{(2)}$ (kcal/mol)	$E_0^{(3)}$ (kcal/mol)	$E_0^{(4)}$ (kcal/mol)	V_{3-4} (kcal/mol)	γ (dimensionless)	$E_0^{(8)}$ (cm^{-1})
1	1.0, 4.16				4	0.5	−40
2	1.0, 3.21				4	0.5	−90
3	1.1, 3.21				4	0.5	30
4	1.1, 2.46				4	0.5	−30
5	1.2, 1.89				4	0.5	0
6	1.0, 4.16				8	0.5	50
7	1.0, 4.16				ho[a]	0.5	100
8	1.0, 4.16				4	1.0	150
9	1.0, 4.16				4	0.25	−275
10	1.0, 4.16	−14			4	0.5	−40
11	1.0, 4.16	−18			4	0.5	−40
12	1.0, 4.16		−6.8	−9.8	4	0.5	160
13	1.0, 4.16		−10.8	−13.8	4	0.5	−280
14	1.0, 4.16				4	0.3	−200

[a] Harmonic oscillator.

larger values of η_{8b} yield larger rate coefficients. For large η_{8b} the increased rate coefficient at low temperature results in a rate coefficient that has a substantial minimum at intermediate temperature. Interestingly, a similar minimum in the $k(T)$ plot has also been calculated for the association of O with OH.[50,51] Such minima in $k(T)$ plots may be indicative of the importance of H-bonding interactions in determining the transition state locations. In particular, at low temperatures (e.g., 300 K) the extra stabilization provided by the H-bonding may push the transition state out to larger separations and thereby yield larger rate coefficients. With increasing temperature the H-bonding interactions would gradually decrease in importance as the corresponding Boltzmann factor $[\exp(-E_{H-bond}/k_BT)]$ approaches unity. At quite high temperature (e.g., $T > 1000$ K) the transition state will have moved in to such short separations that the H-bonding interactions are largely irrelevant. The rate coefficient will then show the usual modest variation with temperature.

We normally expect a rate coefficient such as $k_8^{(c)}$ to be at least 1×10^{13} cm^3/(mol s) at room temperature and to decrease slightly with increased temperature. Furthermore, we generally need small values of $N_8(E,J)$ in order to give good agreement with experiment for $\alpha(T)$. For these reasons, we have presented results in Figure 2 for η_{8a},η_{8b} pairs that have $k_8^{(c)}$(300 K) values near 1×10^{13} cm^3/(mol s). As discussed below, the predicted branching fractions $\alpha(T)$ agree most closely with experiment when there is a significant minimum in the $k_8^{(c)}(T)$ plot. The case (η_{8a}, η_{8b}) = (1.0, 4.16) $Å^{-1}$ satisfies all our criteria. Thus, we have chosen these values for our nominal case.

It is perhaps worth noting that $OH(X^2\Pi)$, because of the orbital symmetry of its electronic wave function, has an abnormally large electronic partition function, approximately by a factor of 1.5 at room temperature. Correcting for this effect makes cases with $k_8^{(c)} < 1 \times 10^{13}$ cm^3/(mol s) somewhat more palatable. Nevertheless we have still chosen $\eta_{8a} = 1.0$ $Å^{-1}$ and $\eta_{8b} = 4.16$ $Å^{-1}$ as our nominal values.

Table 1 lists values of the critical parameters in the calculations for each of the cases discussed here. If no value is given in the table, the value of the parameter given in the Appendix was used for that case. The value of $E_0^{(8)}$ was adjusted for each case so that $\alpha(300\text{ K}) \approx 0.10$, a result that is reasonably well established from experiment. Note that in all these cases, regardless of the changes made to other parameters, reaction b turns out to be thermoneutral to within ±1 kcal/mol. Therefore, it seems reasonable to conclude that the real value of $E_0^{(8)}$ is unlikely to deviate from zero by more than 1 kcal/mol in either direction. Perhaps this is a good test of electronic structure theory results.

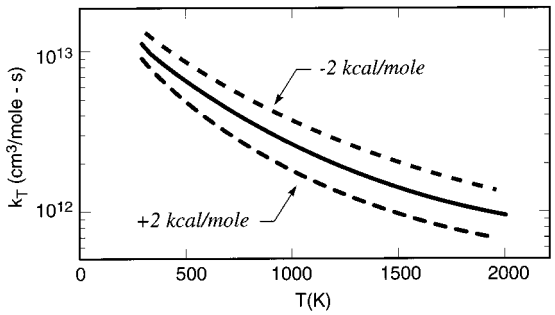

Figure 3. Effect of increasing and decreasing $E_0^{(2)}$ by 2 kcal/mol on $k_T(T)$. The solid line is case 1 of Table 1. The upper dashed line is case 11 and the lower dashed line is case 10.

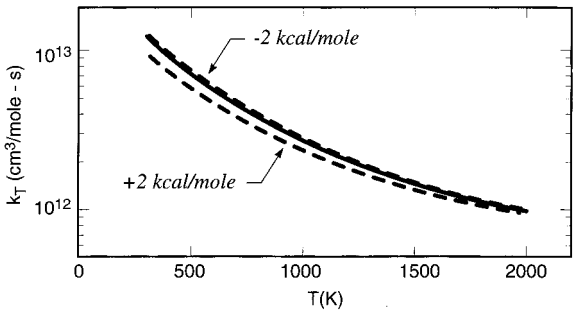

Figure 4. Eeffect on $k_T(T)$ of raising and lowering $E_0^{(3)}$ and $E_0^{(4)}$ in tandem by 2 kcal/mol. The solid line is case 1. The upper dashed line is case 13 and lower dashed line is case 12.

Total Rate Coefficient $k_T(T)$. As noted above, the rate-limiting step in determining $k_T(T)$ is internal rearrangement of the complex $-k_1^{(c)}(T) \approx 2.9-4.5 \times 10^{13}$ cm^3/(mol s) whereas $k_T(T)$ varies from 1×10^{13} cm^3/(mol s) at room temperature to 1×10^{12} cm^3/(mol s) at 2000 K. However, there are two relatively high points in potential energy along the reaction path shown in Figure 1: the 1,3 hydrogen transfer (TS-2), and the trans−cis isomerization, TS-3 and TS-4, which we consider to be a unified pair connected through the torsional motion discussed in the last section. It is instructive to examine which of these transition states has the greater influence on the rate coefficient. Figure 3 is a plot of $k_T(T)$ vs T for our nominal conditions (case 1) and for cases in which $E_0^{(2)}$ was increased and decreased by 2 kcal/mol. Figure 4 is a similar plot in which $E_0^{(3)}$ and $E_0^{(4)}$ were increased and decreased in unison by 2 kcal/mol. Somewhat surprisingly, comparison of the two figures shows that the rate-limiting step is the 1,3 hydrogen shift from the initial NH_2NO complex, particularly at high temperature. This is true even though $E_0^{(4)}$ and $E_0^{(3)}$ are significantly larger

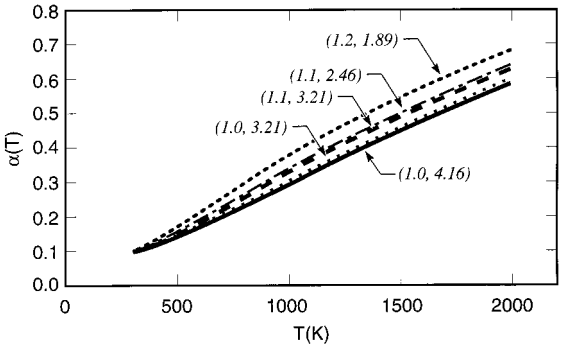

Figure 5. Effect of varying the decay constants η_{8a} and η_{8b} on the branching fraction $\alpha(T)$. The calculations are for cases 1−5. The numbers in parentheses are the values (in Å^{-1}) of η_{8a} and η_{8b}, respectively.

than $E_0^{(2)}$. The tightness of TS-2 severely limits the value of the rate coefficient. This is clear if one compares the frequency values of the low-frequency vibrations of TS-2 with those of TS-3 and TS-4 in the Appendix.

Our value of $E_0^{(2)}$ is −16 kcal/mol. Conventional wisdom usually allows ±2 kcal/mol in the accuracy of the best ab initio electronic structure calculations. If this is so, our value of $E_0^{(2)}$ compares favorably with the −14.8 kcal/mol calculated by Walch[19] and with the −14.4 kcal/mol calculated by Diau and Smith,[20] probably the most accurate of the results obtained to date.

Branching Fraction α(*T*). More interesting than the rate coefficient, and of much more practical importance, is the branching fraction $\alpha(T)$. As discussed by Diau and Smith,[13] the most influential feature of the PES on $\alpha(T)$ is $E_0^{(8)}$ (not surprisingly). We have acknowledged this sensitivity above in adjusting $E_0^{(8)}$ to give $\alpha(300\ \text{K}) \approx 0.10$ for all cases considered. However, other factors also influence the branching fraction. In the following discussion we examine the influence on $\alpha(T)$ of η_{8a}, η_{8b}, V_{3-4} (the torsional barrier separating TS-3 from TS-4), the $E_0^{(3)}$,$E_0^{(4)}$ combination, and γ.

Figure 5 shows $\alpha(T)$ plotted as a function of temperature for various values of η_{8a} and η_{8b}. As expected, $\alpha(T)$ is a strong function of these tightening parameters, at least of η_{8a}. When we compare the predictions of our final theoretical model with experiment below, it will be clear that we want to pick values of all the parameters that give the smallest values of $\alpha(T)$, yet are physically realistic. As discussed above, the case $\eta_{8a} = 1.0$ Å^{-1}, $\eta_{8b} = 4.16$ Å^{-1} results in values of $k_8^{(c)}(T)$ that are in the expected range and also yields the smallest values of $\alpha(T)$. Thus, our preferred values for η_{8a} and η_{8b} are 1.0 and 4.16 Å^{-1}, respectively. Note that in Figure 5 $\alpha(T)$ does not depend strongly on η_{8b}. This is because η_{8b} affects the flux through TS-8 only at low temperature, and our adjustment of $E_0^{(8)}$ to give $\alpha(300\ \text{K}) = 0.1$ for all cases cancels its effect.

Figure 6 displays results for $\alpha(T)$ for two values of the TS-3 → TS-4 torsional barrier, V_{3-4}, and for the case where this torsional motion is modeled as two independent harmonic oscillators. Clearly, the smaller torsional barrier results in the most flux through the trans−cis transition states, and thus smaller values of $\alpha(T)$. However, the differences between the three cases is not huge. Owing to this relative lack of sensitivity to V_{3-4} and our belief that any value of V_{3-4} much smaller than 4 kcal/mol is probably unrealistic, our preferred value is $V_{3-4} = 4$ kcal/mol.

Figure 7 shows the effect of raising and lowering $E_0^{(3)}$ and $E_0^{(4)}$ in tandem by 2 kcal/mol. This is an intriguing plot. The

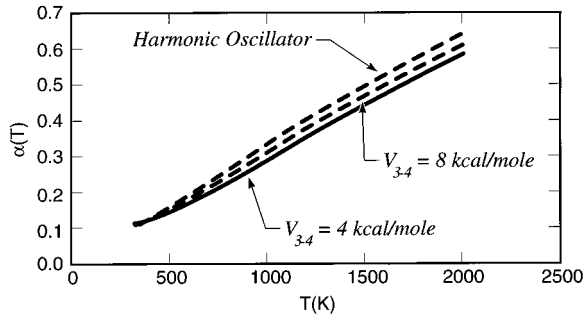

Figure 6. Effect on $\alpha(T)$ of V_{3-4}, the torsional potential barrier separating TS-3 from TS-4. The calculations shown are for cases 1, 6, and 7 of Table 1.

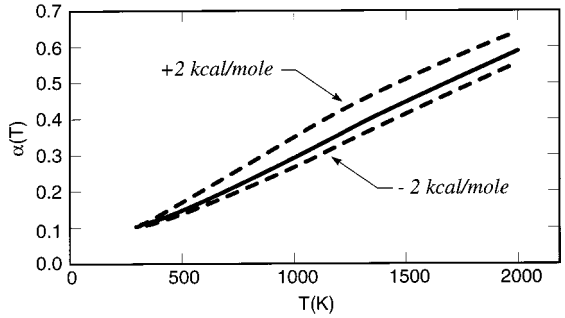

Figure 7. Effect of increasing and decreasing $E_0^{(3)}$ and $E_0^{(4)}$ in tandem by 2 kcal/mol on $\alpha(T)$. The cases shown are case 1, case 12, and case 13.

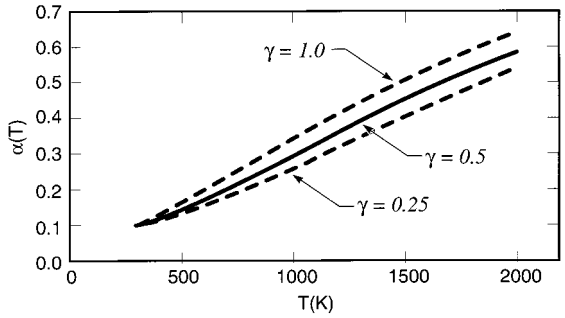

Figure 8. Effect of γ on $\alpha(T)$. The calculations shown are for cases 1, 8, and 9.

smaller we make $E_0^{(3)}$ and $E_0^{(4)}$, the slower is the rise with T of $\alpha(T)$. This result is somewhat counterintuitive and occurs because we adjust the value of $E_0^{(8)}$ in all cases to give $\alpha(300\ \text{K}) \approx 0.10$. The smaller values of $E_0^{(3)}$ and $E_0^{(4)}$ result in smaller values of $E_0^{(8)}$. The smaller values of $E_0^{(8)}$ in turn produce a weaker temperature dependence for $\alpha(T)$ than do larger values of $E_0^{(8)}$. Our values for $E_0^{(3)}$ and $E_0^{(4)}$ are −8.8 and −11.8 kcal/mol, respectively. These numbers compare favorably with the G2M theoretical results of Diau and Smith,[20] $E_0^{(3)} = -8.1$ kcal/mol and $E_0^{(4)} = -10.3$ kcal/mol, and somewhat less favorably with Walch's value of $E_0^{(4)} = -7.4$ kcal/mol. Ultimately we could improve the agreement of our theoretical predictions with experiment by further reducing $E_0^{(3)}$ and $E_0^{(4)}$. However, this would take us further away from the electronic structure theory results than we would like.

In Figure 8 we show the effect of γ on $\alpha(T)$. As expected, larger values of γ (the fraction of $N_8(E,J)$ that connects NNH + OH with complex y) produce larger values of $\alpha(T)$ at high temperature. This occurs because dissociation is not able to compete very favorably with the low energy 1,2 elimination of water from complex z. This sensitivity of $\alpha(T)$ to γ naturally

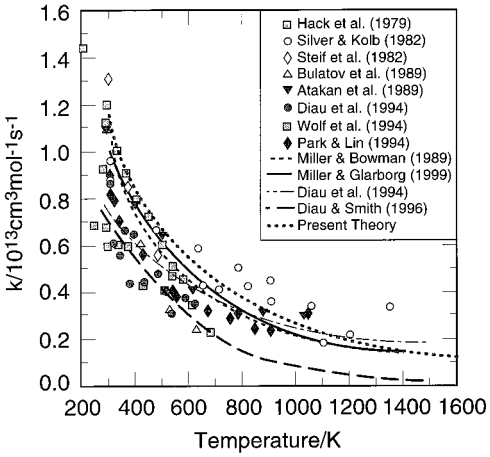

Figure 9. Comparison of our theoretical predictions for $k_T(T)$ with experiment. Case 14, modified as discussed in the text, is used in the predictions.

raises the question of what the correct value of γ should be. It could also be temperature dependent. Only more information about the PES connecting NNH + OH to the y and z complex configurations can clear up this issue. Of course, the noncommittal choice is $\gamma = {}^1/_2$.

We can only speculate on this point, but it seems likely, based on their description of their calculations and our own experience, that the very rapid rise of $\alpha(T)$ with temperature predicted by Diau and Smith[13] is a consequence of implicitly assuming $\gamma = 1$ and taking the equivalent of very large values for the η_{8a},η_{8b} pair. It is quite likely that their equivalent of $k_8^{(c)}$ increases with temperature. A value of unity for γ implies that all the reactive flux through TS-8 originates in complex y. Such an assumption is physically unrealistic.

Comparison of Theory with Experiment for $k_T(T)$ and $\alpha(T)$. We have chosen the conditions listed in Table 1 as case 14 to use in comparing with experiment, except that γ was allowed to increase slowly from the value of 0.3 given in the table at 1100 K to a value of 0.5 at 2000 K. In the absence of any information about this part of the PES, we cannot yet justify such a variation a priori, but some such variation of γ with T is helpful, if not necessary, in predicting the unusual temperature dependence of $\alpha(T)$ observed experimentally (see below).

In Figure 9 we compare our predictions of $k_T(T)$ with the experimental results available. The agreement is very good. The total rate coefficient is determined almost completely by the properties of TS-2, particularly at high temperature. We chose the value of $E_0^{(2)} = -16$ kcal/mol to give a result for k_T(300 K) of approximately 1×10^{13} cm^3/(mol s). The remainder of the prediction occurs naturally. As discussed above, our value for $E_0^{(2)}$ is consistent with the best electronic structure calculations available.

Figure 10 compares our prediction of $\alpha(T)$ with experiment. The branching fraction is much harder to predict than the rate coefficient. The solid curve in Figure 10 is the $\alpha(T)$ function used by Miller and Glarborg[6] in their modeling of the Thermal De-NO_x process; it is probably the most accurate representation of the true $\alpha(T)$ function available. The Miller−Glarborg function changes curvature at $T \approx 1150$ K, a property that is extremely difficult to predict theoretically. In fact, the only way that we can see to produce such an effect quantitatively with the present theoretical treatment is to assume a temperature dependence for γ such as the one described above. To clarify this point we have plotted in Figure 11 the Miller−Glarborg function and the $\alpha(T)$ functions from our nominal case and from

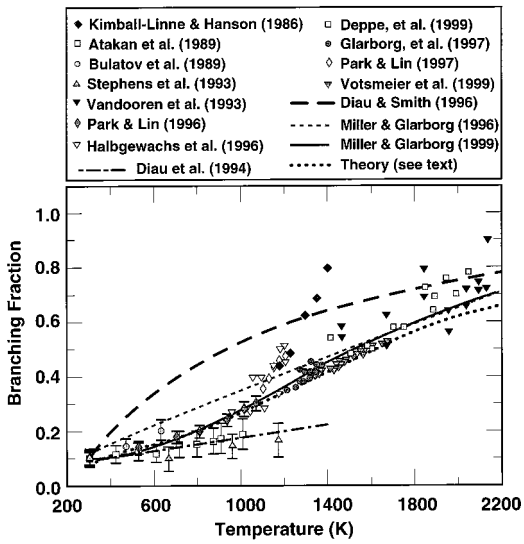

Figure 10. Comparison of our theoretical predictions for $\alpha(T)$ with experiment. Case 14, modified as discussed in the text, is used in the predictions.

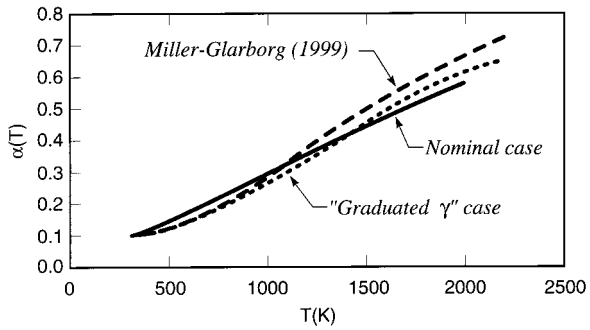

Figure 11. Comparison of our nominal case (case 1) and the "graduated γ " case of Figure 10 with the Miller−Glarborg $\alpha(T)$ function.

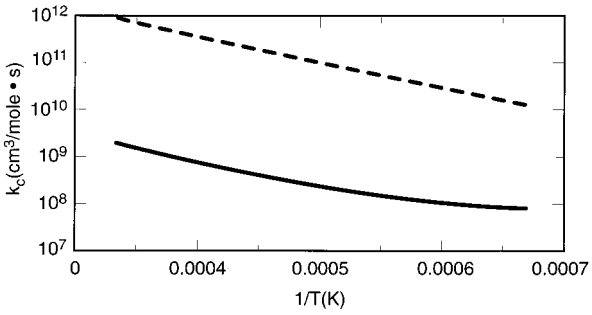

Figure 12. Comparison of our prediction for $k_c(T)$, the rate coefficient for the reaction $NH_2 + NO \rightarrow N_2O + H_2$, with the experiment of Roose et al.[35]

the "graduated γ " case described above. If examined carefully, it can be seen that our nominal case qualitatively displays the change in curvature exhibited by the experiments. This change in curvature correlates directly with the minimum in the $k_8^{(c)}(T)$ function shown in Figure 2 and implies that the forces that produce such a minimum can also lead to the change in curvature in $\alpha(T)$. However, it is only with the temperature-dependent γ that the theoretical $\alpha(T)$ approaches the Miller−Glarborg function.

The N_2O + H_2 Channel. In Figure 12 we compare our prediction for $k_c(T)$

$$NH_2 + NO \rightarrow N_2O + H_2 \qquad (c)$$

with the experimental result of Roose, Hanson, and Kruger.[35]

In the temperature range of interest, our prediction of $k_c(T)$ is between 2 and 3 orders of magnitude smaller than the experimental result. No realistic changes in the properties of TS-6 and TS-7 will bring the two results into agreement. It seems likely that the N_2O detected in the experiments of Roose et al. came indirectly from the channel

$$NH_2 + NO \rightarrow HNNO + H \qquad (d)$$

followed by dissociation or abstraction of the H from HNNO[36] or from secondary reactions such as $NH + NO \leftrightarrow N_2O + H$ and $NH_2 + NO_2 \rightarrow N_2O + H_2O$. Channel d is roughly 39 kcal/mol endothermic, would have a loose (bond fission) transition state, and is accessible from complex x of Figure 1, where it only has to compete with the very tight TS-2.

Concluding Remarks

Using statistical−theoretical methodology, we have studied the $NH_2 + NO$ reaction in some detail. Systematic tests of the sensitivity of $k_T(T)$ and $\alpha(T)$ to various features of the potential energy surface clearly show that $k_T(T)$ is determined almost exclusively by TS-2, the 1,3 hydrogen transfer from the initial NH_2NO complex, whereas $\alpha(T)$ is sensitive to several PES parameters. Our final theoretical model predicts values of $k_T(T)$ and $\alpha(T)$ that agree well with experiment. In order to predict $\alpha(T)$ a priori with any degree of precision, it is clear that more information is needed about the potential governing HNNOH complex formation from the separated NNH + OH fragments. Very subtle features of this part of the potential apparently have significant impact on the shape of the $\alpha(T)$ function. From the present model, we conclude that the potential is likely to have features that produce a $k_8^{(c)}(T)$ function that decreases relatively rapidly with temperature as T increases above 300 K and may have a minimum in the vicinity of $T \approx 1000$ K. Also, the rate of formation of various HNNOH isomers from NNH + OH is probably temperature dependent, with the cis isomers favored at low temperatures.

Our prediction of $k_c(T)$, the rate coefficient for the $N_2O + H_2$ channel, is between 2 and 3 orders of magnitude smaller than that deduced from the experiment by Roose et al.[35] about 20 years ago.

Acknowledgment. This work was supported by the United States Department of Energy, Office of Basic Energy Sciences, Division of Chemical Sciences.

References and Notes

(1) Lyon, R. K. U.S. Patent **1975**, *3*, 900, 554.

(2) Miller, J. A.; Branch, M. C.; Kee, R. J. *Combust. Flame* **1981**, *43*, 81.

(3) Miller, J. A.; Bowman, C. T. *Prog. Energy Combust. Sci*. **1981**, *15*, 287−338.

(4) Miller, J. A.; Glarborg, P. Modeling the Formation of N_2O and NO_2 in the Thermal De-NO_x Process. In *Gas-Phase Chemical Reaction Systems: Experiments and Models 100 years after Max Bodenstein*; Wolfrum, J., Volpp, H.-R., Rannacher, R., Warnatz, J., Eds.; Springer Series in Chemical Physics; Springer: New York, 1996; Vol. 61, pp 318−333.

(5) Miller, J. A. *Twenty-Sixth Symposium (International) on Combustion*; The Combustion Institute: Pittsburgh, PA, 1996; pp 461−480.

(6) Miller, J. A.; Glarborg, P. *Int. J. Chem. Kinet.* **1999**, *31*, 757−765.

(7) Glarborg, P.; Dam-Johansen, K.; Miller, J. A.; Kee, R. J.; Coltrin, M. E. *Int. J. Chem. Kinet*. **1994**, *26*, 421.

(8) Glarborg, P.; Kristensen, P.; Dam-Johansen, K.; Miller, J. A. *J. Phys. Chem. A* **1997**, *101*, 3741−3745.

(9) Park, J.; Lin, M. C. *J. Phys. Chem.* **1996**, *100*, 3317−3319.

(10) Votsmeier, M.; Song, S.; Hanson, R. K.; Bowman, C. T. *J. Phys. Chem. A* **1999**, *103*, 1566−1571.

(11) Selgren, S. F.; McLoughlin, P. W.; Gellene, G. I. *J. Chem. Phys.* **1989**, *90*, 1624.

(12) Koizumi, H.; Schatz, G. C.; Walch, S. P. *J. Chem. Phys.* **1991**, *95*, 4130.

(13) Diau, E. W.-G.; Smith, S. C. *J. Phys. Chem.* **1996**, *100*, 12349−12354.

(14) Melius, C. F.; Binkley, J. S. *Twentieth Symposium (International) on Combustion;* The Combustion Institute: Pittsburgh, PA, 1985; pp 575−583.

(15) Abou-Rachid, H.; Pouchan, C.; Chaillet, M. *Chem. Phys.* **1984**, *90*, 243−255.

(16) Harrison, J. A.; MacIagan, R. G. A.; Whyte, A. R. *J. Phys. Chem.* **1987**, *91*, 6683.

(17) Wolf, M.; Yang, D. L.; Durant, J. L. *J. Photochem. Photobiol. A: Chem.* **1994**, *80*, 85−93.

(18) Duan, X.; Page, P. *J. Mol. Struct. (THEOCHEM)* **1995**, 333, 233−242.

(19) Walch, S. P. *J. Chem. Phys.* **1993**, *99*, 5295−5300.

(20) Diau, E. W.-G.; Smith, S. C. *J. Chem. Phys.* **1997**, *106*, 9236−9251.

(21) Phillips, L. F. *Chem. Phys. Lett.* **1987**, *135*, 269−274.

(22) Lesclaux, R.; Khé, P. V.; DeZauzier, P.; Soulignac, J. C. *Chem. Phys. Lett*. **1975**, *35*, 493.

(23) Gilbert, R. G.; Whyte, A. R.; Phillips, L. F. *Int. J. Chem. Kinet.* **1986**, *18*, 721−737.

(24) Diau, E. W.-G.; Yu, F.; Wagner, M. A. G.; Lin, M. C. *J. Phys. Chem*. **1994**, *98*, 4034.

(25) Troe, J. *J. Chem. Soc., Faraday Trans.* **1994**, *90*, 2303−2317.

(26) Just, Th. *Twenty-Fifth Symposium (International) on Combustion*; The Combustion Institute: Pittsburgh, PA, 1994; pp 687−704.

(27) Varshni, V. P. *Rev. Mod. Phys.* **1957**, *29*, 664−682.

(28) Klippenstein, S. J.; Kundhar, L. R.; Zewail, A. H.; Marcus, R. A. *J. Chem. Phys* **1988**, *89*, 4761−4770.

(29) Miller, J. A.; Parrish, C.; Brown, N. J. *J. Phys. Chem.* **1986**, *90*, 3339.

(30) Pitzer, K. S.; Gwinn, W. D. *J. Chem. Phys.* **1942**, *10*, *428.*

(31) Klippenstein, S. J. *J. Phys. Chem*. **1994**, *98*, 11459−11464 and references therein.

(32) Wardlaw, D. M.; Marcus, R. A. *Chem. Phys. Lett.* **1984**, *110*, 230.

(33) Wardlaw, D. M.; Marcus, R. A. *J. Chem. Phys*. **1985**, *83*, 3462.

(34) Klippenstein, S. J.; Wagner, A. F.; Dunbar, R. C.; Wardlaw, D. M.; Robertson. VARIFLEX Version 0.27, May 19, 1999.

(35) Roose, T. R.; Hanson, R. K.; Kruger, C. H. *Eighteenth Symposium (International) on Combustion*; The Combustion Institute: Pittsburgh, PA, 1981; pp 853−860.

(36) Miller, J. A.; Mitchell, R. E. *Eighteenth Symposium (International) on Combustion*; The Combustion Institute: Pittsburgh, PA 1981; p 860.

(37) Kimball-Linne, M. A.; Hanson, R. K. *Combust. Flame* **1986**, *64*, 377.

(38) Vandooren, J.; Bian, J.; van Tiggelen, P. J. *Combust. Flame* **1994**, *98*, 402.

(39) Brown, M. J.; Smith, D. B. *25th Symposium (International) Combustion*; The Combustion Institute: Pittsburgh, PA, 1994; p 1011.

(40) Stief, L. J.; Brobst, W. D.; Nava, D. F.; Borkowski, R. P.; Michael, J. V. *J. Chem. Soc., Faraday Trans. 2* **1982**, *78*, 1391.

(41) Atakan, B.; Jacobs, A.; Wahl, M.; Weller, R.; Wolfrum, J. *Chem. Phys. Lett.* **1989**, *155*, 609.

(42) Bulatov, V. P.; Ioffee, A. A.; Lozovsky, V. A.; Sarkisov, O. M. *Chem. Phys. Lett.* **1989**, *161*, 141.

(43) Stephens, J. W.; Morter, C. L.; Farhat, S. K.; Glass, G. P.; Curl, R. F. *J. Phys. Chem.* **1993**, *97*, 8944−8951.

(44) Silver, J. A.; Kolb, C. E. *J. Phys. Chem.* **1982**, *86*, 3249.

(45) Unfried, K. G.; Glass, G. P.; Curl, R. F. *Chem. Phys. Lett.* **1990**, *173*, 337.

(46) Hack, H.; Schacke, H.; Schroeter; Wagner, H. Gg. *Seventeenth Symposium (International) on Combustion*; The Combustion Institute: Pittsburgh, PA, 1979; p 505.

(47) Park, J.; Lin, M. C. *J. Phys. Chem. A.* **1997**, *101*, 5−13.

(48) Halbgewachs, M. J.; Diau, E. W.-G.; Mebel, A. M.; Lin, M. C.; Melius, C. F. *Twenty-Sixth Symposium (International) on Combustion*; The Combustion Institute: Pittsburgh, PA, 1996; pp 2109−2115.

(49) Deppe, J.; Friedrichs, G.; Römming, H.-J.; Wagner, H. Gg. *Phys. Chem. Chem. Phys.* **1999**, *1*, 427.

(50) Miller, J. A.; Garrett, B. C. *Int. J. Chem. Kinet.* **1997**, *29*, 275−287.

(51) Miller, J. A.; Klippenstein, S. J. *Int. J. Chem. Kinet.* **1999**, *31*, 753−756.

Appendix: Nominal Transition-State Properties

transition state	threshold energies $E^{(0)}$ (kcal/mol)	vibrational frequencies (cm^{-1})	principal moments of inertia (amu $bohr^2$)
2	−16	534, 972, 1182, 1210, 1375, 1497, 2180, 3573	26.0, 120.7, 146.7
3	−8.8	3919, 3724, 1783, 1324, 776, 583, 556, 363	23.9, 149.8, 173.7
4	−11.8	3938, 3860, 1836, 1290, 716, 546, 496, 418	22.2, 157.3, 179.5
5	−23.4	3825, 2198, 1858, 1161, 981, 807, 532, 187	34.5, 158.0, 190.8
6	2.6	769, 776, 1118, 1220, 1297, 1471, 1898, 2066	24.6, 128.4, 153.1
7	28.8	279, 547, 900, 1134, 1194, 1323, 1643, 2664	25.5, 131.8, 154.9